Spectral-domain optical coherence phase microscopy for quantitative phase-contrast imaging

Joo, C.; Akkin, T.; Cense, B.; Park, B. H.; de Boer, J.F.

published in
Optics Letters
2005

DOI (link to publisher)
10.1364/OL.30.002131

document version
Publisher's PDF, also known as Version of record

Spectral-domain optical coherence phase microscopy for quantitative phase-contrast imaging

Chulmin Joo

Department of Mechanical Engineering, Massachusetts Institute of Technology, Cambridge, Massachusetts 02139, and Wellman Center for Photomedicine, Massachusetts General Hospital, Boston, Massachusetts 02114

Taner Akkin, Barry Cense, Boris H. Park, and Johannes F. de Boer

Wellman Center for Photomedicine, Massachusetts General Hospital, Boston, Massachusetts 02114

Received February 22, 2005

We describe a novel microscopy technique for quantitative phase-contrast imaging of a transparent specimen. The technique is based on depth-resolved phase information provided by common path spectral-domain optical coherence tomography and can measure minute phase variations caused by changes in refractive index and thickness inside the specimen. We demonstrate subnanometer level path-length sensitivity and present images obtained on reflection from a known phase object and human epithelial cheek cells. © 2005 Optical Society of America

OCIS codes: 110.0180, 110.4500, 120.3180, 170.1530, 180.3170.

Quantitative knowledge of the structures and dynamics of a transparent specimen is of great importance in fields ranging from material inspection[1] to cell biology.[2] Conventional phase-contrast microscopes produce high-contrast qualitative images of transparent objects, but they cannot be directly applied to quantitative studies. Phase-shifting interferometry[3] is commonly used to produce two-dimensional quantitative phase distribution of a sample. However, it requires a sophisticated device to generate the four interferograms with precisely controlled phase difference between the reference and sample fields. Cuche *et al.* presented digital holography for quantitative phase-contrast imaging. It uses a CCD camera for hologram recording and a numerical method for hologram reconstruction.[4] A noninterferometric phase-extraction technique was also demonstrated, but it needs displaced intensity measurements made by moving a sample along the optical axis.[5] Quantitative phase-sensitive microscopes based on dual-channel low-coherence interferometers were recently reported.[6,7] Both schemes measure subwavelength optical path-length (OPL) variations in two-dimensional space by using the phase difference between two orthogonal polarization channels.

We present a novel quantitative phase imaging modality, referred to as spectral-domain optical coherence phase microscopy (SD-OCPM). The technique is based on spectral-domain optical coherence tomography[8,9] to produce depth-resolved intensity and phase profiles with significantly improved phase stability compared with those of time-domain OCT based systems.[10–12] Because SD-OCPM acquires depth-resolved information without mechanical scanning of the reference mirror, it can generate a three-dimensional quantitative phase-contrast image of a specimen simply by scanning the beam laterally as it measures phase profiles in depth. In this Letter we present, as an initial demonstration, the application of SD-OCPM to two-dimensional quantitative phase-contrast imaging in reflection. We show subnanometer OPL sensitivity of the system and then compare images of a known phase sample and human epithelial cells with those from conventional Nomarski microscopy.

Figure 1 depicts an experimental setup of SD-OCPM, which includes a fiber-based common-path spectral-domain optical coherence tomography interferometer. A broadband 840 nm superluminescent diode (50 nm FWHM) is employed as the light source, and the beam is delivered to a specimen by a custom-built microscope equipped with a lateral beam scanner and a microscope objective (Carl Zeiss; 20×; N.A., 0.5). The $1/e^2$ diameter of the incident beam to the objective was ~3.4 mm, giving an effective N.A. of 0.2. The lateral resolution was measured as 2.6 μm (FWHM). In our method the reflection from the top surface of a coverslip serves as the reference optical field,[8,12] whereas the backscattered waves from the sample are the measurement fields [Fig. 1(b)]. Because the thickness of the coverslip (~220 μm) is larger than that of the target sample such as a cell (<100 μm), the interference signal referenced to the

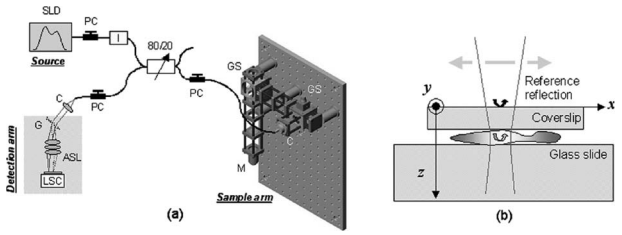

Fig. 1. (a) Schematics of the SD-OCPM system: SLD, superluminiscent diode; PCs, polarization controllers; I, isolator; 80/20, 80/20 fiber-based beam splitter; G, transmission grating; ASL, three-element air-spaced lens; LSC, line scan camera; C, collimator; GS, galvanometer scanner; M, microscope objective. (b) Sample placed between a coverslip and a microscope slide. SD-OCPM measures phase distribution of a sample referenced to the top surface of the coverslip.

0146-9592/05/162131-3/$15.00

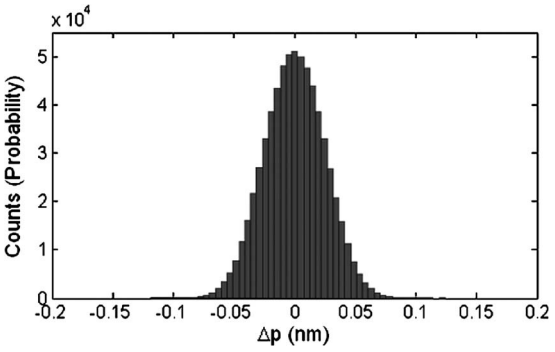

Fig. 2. Probability distribution of measured phase sensitivity. The experiment was performed for ~21 s, and the standard deviation was 25 pm. The measured SNR was 100.4 dB.

top surface of the coverslip can be distinguished easily from the interference signals referenced to other surfaces. The interference signals are detected by a high-speed spectrometer, acquiring 29,200 depth profiles per second continuously with a 98% duty cycle.[9]

If the beam is positioned at (x,y) over a sample, the intensity related to the interference is given by

$$I(k)|_{(x,y)} = 2[R_r R_s(z)]^{1/2} S(k) \cos(2k\Delta p)|_{(x,y)}, \quad (1)$$

where k is the free-space wave number, z is the geometrical distance, and R_r and R_s represent the reference reflectivity and sample reflectivity at depth z, respectively. $S(k)$ is the source power spectral density, and Δp is the OPL difference between the reference and sample beams. A complex-valued depth profile $F(z)$ is obtained by a discrete Fourier transform of Eq. (1) with respect to $2k$, so we can extract the phase as a function of z by taking the argument of $F(z)$:

$$\phi(z)|_{(x,y)} = \tan^{-1}\left\{\frac{\mathrm{Im}[F(z)]}{\mathrm{Re}[F(z)]}\right\} = 2\frac{2\pi}{\lambda_0}\Delta p(z), \quad (2)$$

where λ_0 is the center wavelength of the source. The depth-resolved phase measurement is performed as the beam scans laterally across the sample. Therefore, SD-OCPM is capable of producing phase-contrast images of the samples at depth z. The image is quantitative relative to the reference surface, which is the top surface of a coverslip in our case.

Phase sensitivity is an important performance factor in SD-OCPM, as it determines the ability of the system to detect phase changes spatially and temporally. The spatial phase changes are induced by the spatial refractive-index gradients and the variations of geometric size of the structures, and the temporal phase sensitivity is defined as the ability to detect minute variations of the reflector's position in time. The phase sensitivity can be characterized by the variance (or the standard deviation) of the phase, and it is expressed as an explicit function of the signal-to-noise ratio (SNR) as $\langle \Delta\phi^2 \rangle \approx 1/(2\mathrm{SNR})$.[12,13] To quantify the phase sensitivity of SD-OCPM we measured the phase related to the interference of the top and bottom surfaces of a coverslip. Figure 2 shows a histogram based on the measurement performed for ~21 s. The measured SNR was 100.4 dB, under which condition the theoretical sensitivity is 0.4 pm. The measured sensitivity in SD-OCPM was 25 pm in air. The difference between the theoretical and measured sensitivities may be due to the influence of external disturbances such as vibrations in the coverslip during the measurement.

To demonstrate the imaging performance of SD-OCPM, we imaged the letters "MGH" on a coverslip. The etch depth in the sample was measured as ~62 nm by a surface profiler (Dektak 3030), which corresponds to an expected OPL of ~94 nm in air for a refractive index of the coverslip of 1.51. For imaging, the phase of the interference between the reflections from the top and bottom surfaces of the etched coverslip was measured as the beam was scanning laterally. The measured phase was converted to the OPL difference in air, and we obtained the physical depth information by dividing the OPL by the refractive index of the coverslip. Figure 3 shows the images of the sample recorded by a Nomarski microscope (10×; N.A., 0.3) and SD-OCPM. The gray scale in the SD-OCPM image denotes the depth with reference to the flat (not etched) surface, in nanometers. The improved contrast in the SD-OCPM image is noticeable. Figure 3(c) shows the etch depth profile of the coverslip in three dimensions. The SD-OCPM measurement corresponds to that of the profiler within 5 nm.

SD-OCPM was also applied to image human epithelial cheek cells. The cells were placed between a coverslip and a microscope glass slide, and the microscope measured the phase of the interference between the top surfaces of the coverslip and the glass slide to examine the *en-face* phase image of the cell in reflection. Figure 4 shows the Nomarski and SD-OCPM images. Note that the cell imaged by the Nomarski microscope shown in Fig. 4(a) is not of the same epithelial cell as in Fig. 4(b). In the case of Fig. 4(b), the *en-face* phase image was unwrapped by Flynn's minimum-discontinuity algorithm.[14,15] Along with the *en-face* phase-contrast image, we plotted the surface map of the phase image to show the optically thick nuclei and subcellular structures in a three-dimensional representation. The cell membrane, nucleus, and some other subcellular structures are visible. Two cheek-cells seem to be superimposed,

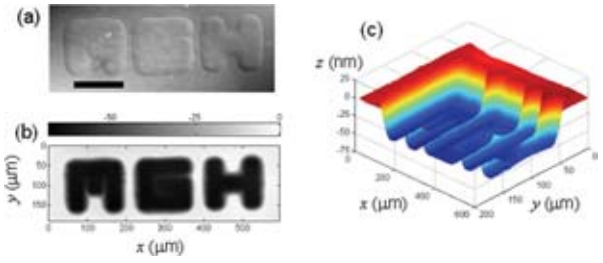

Fig. 3. Images of the letters MGH on a coverslip. (a) Image recorded by Nomarski microscope (10×; N.A., 0.3). The solid bar corresponds to 125 μm. (b) Image taken by SD-OCPM. The gray scale represents the etch depth in nanometers. (c) Three-dimensional etch depth profile of the patterned coverslip.

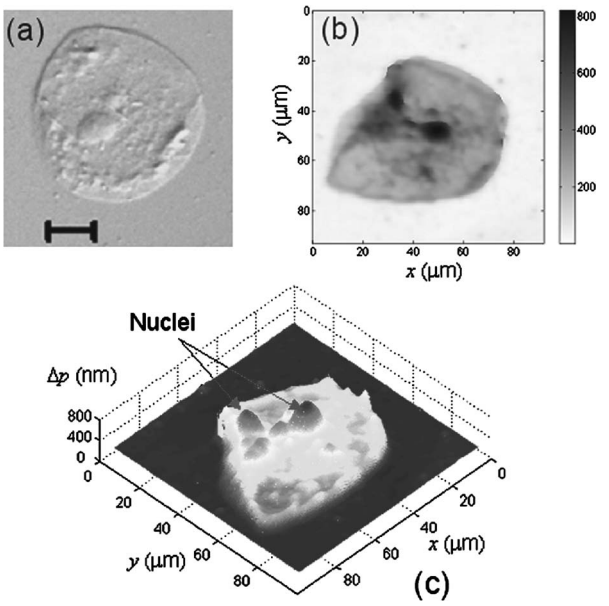

Fig. 4. Images of human epithelial cheek cells. (a) Image recorded by a Nomarski microscope (10×; N.A., 0.3); the bar represents 20 μm. (b) SD-OCPM image, along with the gray scale denoting the OPL in nanometers. (c) Surface plot of (b), showing optically thick structures such as nuclei and subcellular structures in the cell. The nuclei and subcellular structures are visible, and two cells seem to be overlapping, based on the presence of two nuclei in the image.

based on the appearance of two nuclei in the image. The image contains 350×300 pixels, and the total acquisition time was 3.6 s.

The extension of SD-OCPM to three-dimensional quantitative phase imaging necessitates higher axial resolution. The current axial resolution of SD-OCPM, which is limited by the spectral bandwidth of the source, is ~8 μm (FWHM) in air and so does not provide enough resolution for examination and discrimination of subcellular structures in depth in a 10 to 15 μm thick cell. Therefore the use of the source with a broader spectrum will enable us to resolve smaller structures within the sample, eventually allowing for three-dimensional quantitative phase-contrast imaging. The lateral resolution of SD-OCPM, however, can be improved either by use of a higher-N.A. objective or by an increase in the size of the beam incident onto the objective lens.

In summary, a fiber-based spectral-domain optical coherence phase microscope was developed for quantitative phase-contrast imaging. Based on the features of a common-path spectral-domain optical coherence tomography interferometer, the microscope can record spatial and temporal OPL changes quantitatively. The phase sensitivity of a SD-OCPM has an explicit relationship with the SNR of the backscattered interference signal, and subnanometer sensitivity for a good reflector was demonstrated. Two-dimensional quantitative phase-contrast images in reflection were also presented. This technique can easily be extended to serve as a three-dimensional quantitative phase-contrast imaging tool by use of a source with a broader spectrum.

This research was supported in part by research grants from the National Institutes of Health (R01 RR19768, EY14975) and the U.S. Department of Defense (F4 9620-01-1-0014) and by a gift from Dr. and Mrs. J. S. Chen to the optical diagnostics program of the Wellman Center for Photomedicine. C. Joo's e-mail address is cmjoo@mit.edu.

References

1. A. Roberts, E. Ampem-Lassen, A. Barty, K. A. Nugent, G. W. Baxter, N. M. Dragomir, and S. T. Huntington, Opt. Lett. **27**, 2061 (2002).
2. C. Yang, A. Wax, M. S. Hahn, K. Badizadegan, R. R. Dasari, and M. S. Feld, Opt. Lett. **26**, 1271 (2001).
3. K. Creath, Prog. Opt. **26**, 349 (1988).
4. E. Cuche, F. Bevilacqua, and C. Depeursinge, Opt. Lett. **24**, 291 (1999).
5. A. Barty, K. A. Nugent, D. Paganin, and A. Roberts, Opt. Lett. **23**, 817 (1998).
6. M. Sticker, M. Pircher, E. Gotzinger, H. Sattmann, A. F. Fercher, and C. K. Hitzenberger, Opt. Lett. **27**, 1126 (2002).
7. C. Rylander, D. Dave, T. Akkin, T. E. Milner, K. R. Diller, and A. J. Welch, Opt. Lett. **29**, 1509 (2004).
8. A. F. Fercher, C. K. Hitzenberger, G. Kamp, and S. Y. Elzaiat, Opt. Commun. **117**, 43 (1995).
9. N. Nassif, B. Cense, B. H. Park, S. H. Yun, T. C. Chen, B. E. Bouma, G. J. Tearney, and J. F. de Boer, Opt. Lett. **29**, 480 (2004).
10. R. Leitgeb, L. F. Schmetterer, M. Wojtkowski, C. K. Hitzenberger, M. Sticker, and A. F. Fercher, Proc. SPIE **4619**, 16 (2002).
11. B. R. White, M. C. Pierce, N. Nassif, B. Cense, B. H. Park, G. J. Tearney, B. E. Bouma, T. C. Chen, and J. F. de Boer, Opt. Express **11**, 3490 (2003).
12. M. A. Choma, A. K. Ellerbee, C. Yang, T. L. Creazzo, and J. A. Izatt, Opt. Lett. **30**, 1162 (2005).
13. B. H. Park, M. C. Pierce, B. Cense, S. H. Yun, M. Mujat, G. J. Tearney, B. E. Bouma, and J. F. de Boer, Opt. Express **13**, 3931 (2005).
14. T. J. Flynn, J. Opt. Soc. Am. A **14**, 2692 (1997).
15. D. C. Ghiglia and M. D. Pritt, *Two-Dimensional Phase Unwrapping: Theory, Algorithms, and Software* (Wiley, 1998).